J Mater Sci (2011) 46:3399–3404
DOI 10.1007/s10853-010-5228-3

Efficient fabrication of highly conductive and transparent carbon nanotube thin films on polymer substrates

Gaozhi Xiao · Ye Tao · Jianping Lu · Zhiyi Zhang · David Kingston

Received: 21 September 2010 / Accepted: 28 December 2010 / Published online: 7 January 2011

Abstract This paper reports an efficient solution dip coating method for the fabrication of highly transparent and conductive single-walled carbon nanotubes (SWCNTs) based thin films. The key to achieve this is properly preparing the polymer surfaces. In this paper we report a surface pretreatment approach of combining air plasma treatment and silane water solution rinsing for polyethylene terephthalate substrate. After this surface pretreatment, one dip (using a home-made dip coater) of SWCNT solution can yield a thin film of the sheet resistance less than 100 ohms/square (Ω/□) and transparency around 90% at the wavelength of 550 nm; while two dips can produce a thin film of the sheet resistance less than 80 Ω/□ and transparency around 80% at the wavelength of 550 nm. The carbon nanotube thin film performances achieved are close to those of the ITO coatings reported in the literature and the process developed is suitable for both mass production and lab sample preparations.

Introduction

With the emerging of flexible displays and solar cells, highly transparent and conductive flexible electrodes will potentially be in great demand. This type of flexible electrodes is usually fabricated by depositing conductive thin films on flexible polymer substrates. Semiconducting metal oxides, such as indium tin oxide (ITO), are currently the preferred choice as they offer both low electrical resistivity and high transparency in the visible region. However, metal oxides are inherently brittle and tend to lose its conductivity after stretch or bend [1–3]. Recent study by Na et al. [1] found that the resistance of ITO deposited on polyethylene terephthalate (PET) increased by ~40 times after ~2500 bending cycles at a radius of ~8 mm. On the other hand, polymer and carbon nanotube (CNT) conductive coatings have shown great potential in tackling this issue [1, 4, 5].

Many techniques have been explored to fabricate transparent CNT conductive thin films on polymer substrates [4, 6–12], such as printing [6], spraying [7, 8], electrophoretic depositing [9], casting [10], vacuum filtration [11], spin coating [12], layer-by-layer nano assembly [13] and dip coating [4]. Andrade et al. [14] compared the electrical properties of transparent CNT thin films prepared by dip coating, spraying, vacuum filtration and electrophoretic deposition. Their results show that the CNT coating prepared by dip coating method yields the best electrical and optical performance combination. In addition, dip coating renders a much smooth surface compared to that from spraying. The roughness of CNT coating might play an important role for solar cell applications, because in thin layered configurations, rough CNT network could cause a short circuit. However, these authors also found that it is very difficult to dip coat the PET substrate with CNT water solution and multi dipping cycles are needed for achieving a good conductive film. Ng et al. [4] tried to improve this tedious and time-consuming dipping process by pre-treating the PET surfaces with 1,2-aminopropyltriethoxylsilane, but it still needs five coats to obtain a sheet resistance of 2.05 kΩ/□ and film transparency of 84% at the wavelength of 550 nm.

The difficulty in coating the PET surface with CNT is believed due to the surface property mismatching between these two types of materials. CNTs are hydrophobic, while

G. Xiao (✉) · Y. Tao · J. Lu · Z. Zhang · D. Kingston
National Research Council, 1200 Montreal Road, Ottawa, ON K1A 0R6, Canada
e-mail: George.Xiao@nrc-cnrc.gc.ca

PET surface is much more hydrophilic. Therefore, very small amount of CNTs are deposited in each dipping cycle. In this paper, we report a very efficient dip coating process for the fabrication of transparent single-walled carbon nanotube (SWCNT) thin films on the flexible PET film surfaces. By treating the PET surfaces using air plasma followed by the coating of 3-aminopropyltrimethoxylsilane, we are able to produce uniform SWCNT coatings on PET substrate. One dip coat at the room temperature can produce a SWCNT thin film with the sheet resistance less than 100 Ω/□ and film transparency around 90% at the wavelength of 550 nm, while two dip coats can produce a SWCNT thin film with the sheet resistance less than 80 Ω/□ and film transparency around 80% at the wavelength of 550 nm.

Experimental

Materials

SWCNTs were obtained from the Chinese Academy of Sciences. The tubes are of >90% purity and with an outer diameter between 1 and 2 nm and their lengths are varied from 5 to 30 μm. 3-Aminopropyltrimethoxylsilane (APTMS) (97% purity), surfactant Triton X-100 and HNO_3 acid (70% purity) were purchased from Sigma-Aldrich. Anhydrous ethanol was obtained from Commercial Alcohols, Inc.

Several SWCNT water solutions were prepared with the help of magnetic stir and sonication. 1% Surfactant Triton X-100 was added to assist the dispersion of 0.1% SWCNT in water. The solutions were then purified by centrifuge treatment for the purpose of removing the particles and impurities.

The substrate used in this study was a commercial available PET film from DuPont with the trade name of Mylar.

Surface pre-treatment and coating procedures

PET cleaned by ethanol wiping is treated in the plasma chamber (Harrick Plasma Cleaner) under the pressure of ~150 torr for 10 min. The power setting selected is high. The plasma treated films were then dip coated with 1% 3-aminopropyltrimethoxysilane water solution and blow dried in air. The treated films were further dried in a Fisher isotherm oven at the temperature of 110 °C for 10 min.

The dip coating process was conducted in a fume hood using a home build dip coater. One dip coating cycle including the following steps: firstly, the treated PET films were immersed in the SWCNT solution for 10 s and then withdrew at a speed of 0.5 cm/min; secondly, the coated samples were baked in the above mentioned oven at the temperature of 110 °C for 5 min; thirdly, the baked samples were immersed in HNO_3 for 15 s and washed by tap water; finally, the samples were blow dried in air. The whole dipping cycle can be repeated depending on the requirements.

Measurement and analysis

A Kratos Axis Ultra XPS equipped with a non-monochromated Al X-ray source ($hv = 1486.6$ eV) was used to analyze the surface chemical structural changes induced by the surface preparation procedures. Two analyses were performed on each sample. Both were carried out using an accelerating voltage of 14 kV and a current of 10 mA. Charge build-up was compensated for using the Axis charge balancing system. The pressure in the analysis chamber during the work was 2.0×10^{-9} torr. Analyses consisted first of a survey scan performed at a pass energy of 160 eV to identify all the species present, followed by high resolutions scans (40 eV) of the species identified by the survey scan. The energy step is 0.1 eV. Peak assignments were based on the NIST database [15], High resolution XPS of organic polymers (1992) [16] and relevant publications [17, 18]. Peak fitting was performed using CasaXPS (ver. 2.2.107) data processing software. Shirley background correction procedures were used as provided by CasaXPS. Curve fitting procedures used for high resolution spectra presented in this paper used a Gaussian (70)–Lorentzian (30) function. High resolution analyses were calibrated to adventitious C_{1s} signal, at 285 eV. Quantification was performed using sensitivity factors provided by CasaXPS's Scofield element library.

The sheet resistances of the solution prepared samples were measured using a four-point probe measurement method. Each data reported is the average of at least five measurements at different spots with a minimum of 5 mm distance between them.

The optical transmission profiles of the prepared samples were measured with a Varian Cary 50 Bio UV–vis spectrophotometer. The wavelength range measured is from 200 to 800 nm.

The surface morphology of the SWCNT thin film prepared was analyzed by a Hitachi S-4700 field emission scanning electron microscopy (FE-SEM) with a 3 kV acceleration voltage.

Results and discussions

Figure 1 compares the sheet resistances of the SWCNT films dip coated on the PET substrates prepared by varying methods. The results clearly show that using APTMS to

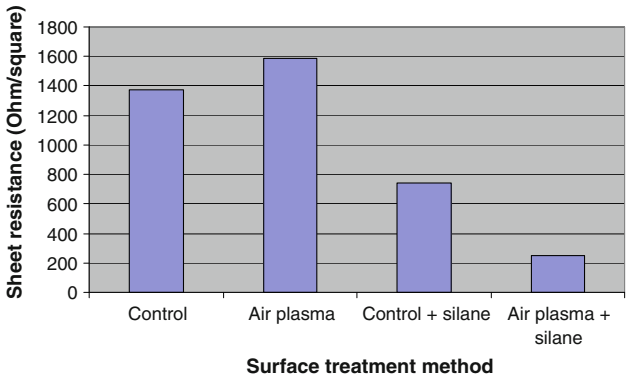

Fig. 1 Sheet resistances of SWCNT coated on pre-treated PET films

treat PET surface can improve the coating efficiency of SWCNT on PET surface, confirming the findings by Ng et al. [4]. The table also shows that air plasma treatment alone does not help the coating efficiency. However, air plasma treatment plus APTMS treatment can significantly improve the dip coating efficiency. If a proper SWCNT solution is used, less than 100 Ω/□ sheet resistance can be achieved after a single dip. This significantly improves the fabrication efficiency and suitability for the mass commercial productions or laboratory fabrication of SWCNT thin films.

To elucidate the mechanism behind this, XPS analyses were carried out for the control and treated PET substrates. Table 1 lists the surface elemental ratios of PET substrate with or without plasma treatments. The control sample has an elemental ratio of 73% carbon, 26% oxygen and 1% nitrogen, which is in good agreement with the expected stoichiometry of PET (71.5% carbon and 28.5% oxygen). The presence of nitrogen and the excess carbon shown on the PET substrate are most probably due to contamination. On the other hand, the high resolution C_{1s} and O_{1s} spectra for the control sample, as shown in Figs. 2a and 3a are also in good agreement with those reported in Ref. [17, 18]. The C_{1s} spectrum for the control sample exhibits four distinct components: the carbon atoms of the phenyl ring (285.00 eV); the methylene carbon atoms singly bonded to oxygen C–O (286.63 eV), and the ester carbons O–C=O (288.96 eV) and π–π^* shake-up peaks associated with the aromatic ring (291.33 and 295.82 eV). While the O_{1s} spectrum for the control sample consists of a doublet and satellite peaks at the higher binding energy, which correspond to the O–C (531.80 eV), O=C component (533.39 eV) in the PET structure and the π–π^* shake-ups (535.22 and 538.47 eV) induced by the phenyl ring.

Table 1 Changes of element ratios of PET after surface treatment measured by XPS

	Percentage of the elements				Element ratio	
	Carbon	Oxygen	Nitrogen	Silicon	O/C	N/C
Control	73.1	25.9	1.0	0.0	0.35	0.01
Air plasma	62.9	32.5	4.6	0.0	0.52	0.07
Control + silane	70.5	26.7	2.8	0.0	0.38	0.04
Air plasma + silane	52.8	24.1	10.0	13.1	0.46	0.19

The data shown in Table 1 clearly demonstrates that the air plasma treatment significantly increases the oxygen and nitrogen amounts on the PET surface. This is in good agreement with the results reported by Yang et al. [19]. Details about air plasma and its interactions with polymer surfaces can be found in Ref. [20]. The results indicate that new functional groups have been introduced to the PET surface by plasma treatment. Changes in the C_{1s} and O_{1s} spectra shown in Figs. 2b and 3b confirm this. It was noted that the binding energy of deconvoluted peaks may not be constant. This is believed to be due to the residual stress, similar to the case being discussed in Ref. [21, 22]. Deposition of APTMS on the control PET sample has slightly increased the oxygen and nitrogen amounts, while no silicon was detected on the samples. This result is a bit surprising, but it probably suggesting that a very small amount of APTMS was coated on the control sample. The area analyzed by XPS probably has very few APTMS on it. On the other hand, the APTMS coated plasma treated PET surface shows the atomic ratio of C:O:N:Si as 52.8:24.1:10.0:13.1 comparing to the stoichiometry of APTMS of 54.5:27.3:9.1:9.1. The results suggest that the air plasma treated surface is covered by APTMS to a very large extent. In addition, APTMS coating greatly modified the C_{1s} and O_{1s} spectra of air plasma treated PET surface (comparing Figs. 2b, d, 3b, d). Specifically, only one type of O_{1s} (Fig. 2d) can be found on the treated surface indicating the significant coverage (if not completely) of APTMS on the plasma treated PET surface.

Water contact angles of PET surfaces before and after surface treatment were also measured. The results of five measurements on each sample are reported in Table 2. It can be seen that plasma treatment makes the PET surface significantly more hydrophilic, while APTMS only treatment makes the PET surface more hydrophobic, suggesting that APTMS might make the PET surface more coatable by SWCNT, which is hydrophobic. Nevertheless, after both air plasma and APTMS treatments, the PET surface has the same water contact angle as that of the control sample, suggesting that the improved dip coat efficiency is not completely due to the change of surface hydrophilicity as suggested by Ng et al. [4].

Combining the XPS and contact angle results, it can be concluded that the coverage of APTMS on PET surface plays an important role on the improvement of SWCNT coating

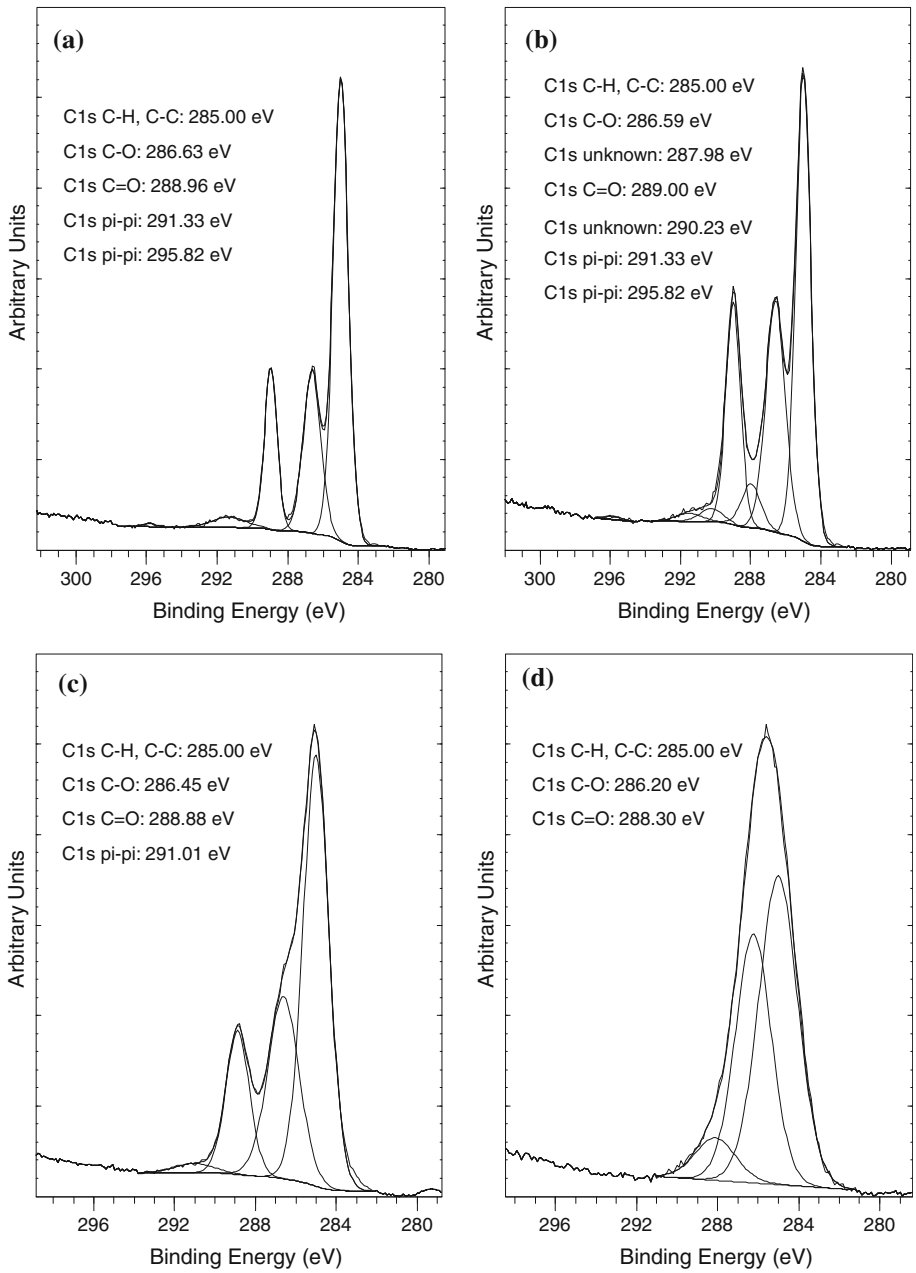

Fig. 2 Comparison of C_{1s} spectra of PET after surface treatment. **a** Control, **b** Air plasma, **c** Control + silane, **d** Air plasma + silane

efficiency. Air plasma treatment introduces functional groups onto the PET surface and improves its wettability, thus making APTMS water solution (1% concentration) much easier to spread on the PET surface. This leads to the significantly improvement of the APTMS coverage on PET surface and hence a better coating efficiency than APTMS alone treated PET substrate.

Several types of SWCNT water solutions were prepared and coated on air plasma and APTMS treated PET substrates. Figure 4 shows the transmission spectra of two of the dip coated samples. Sample A is dip coated once. It has a sheet resistance of $\sim$100 Ω/□ and film transparency of around 90% at the wavelength of 550 nm. Sample B is dip coated twice. It has a sheet resistance of $\sim$70 Ω/□ and film transparency of around 80% at the wavelength of 550 nm. These results are significantly better than those reported in the literature [4, 14], and close to those of the commercial available ITO thin films deposited on PET, such as the ones from Sigma-Aldrich (35 Ω/□, >86% transmission at 550 nm).

Although the pure SWCNT thin films prepared in this work look very smooth under the naked eyes, the thin films are actually SWCNT tangled together with many voids in between at the nanometer scale as the SEM picture shown

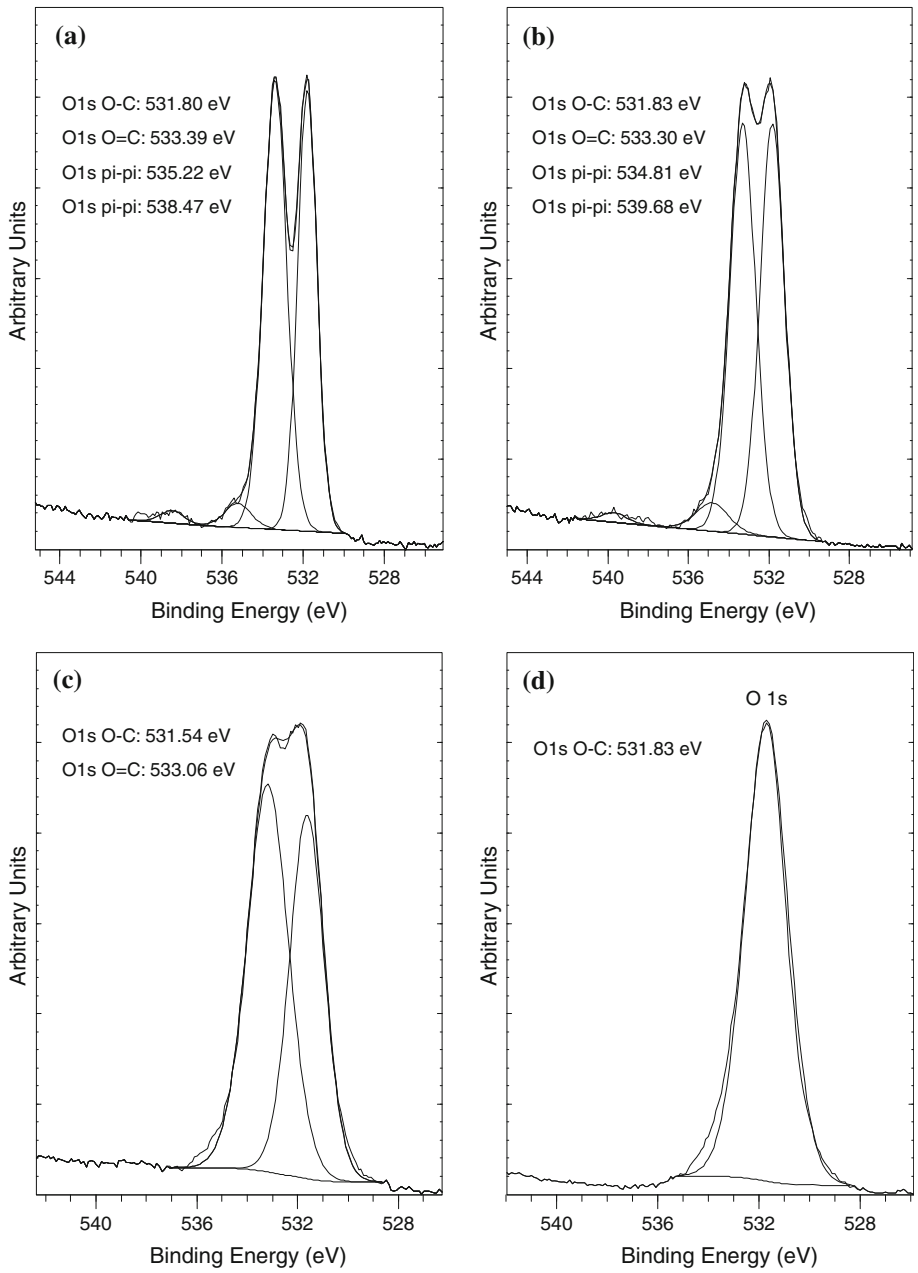

Fig. 3 Comparison of O_{1s} spectra of PET after surface treatment. **a** Control, **b** Air plasma, **c** Control + silane, **d** Air plasma + silane

Table 2 Wettability changes of PET surface after treatment

	Contact angle of DI water (°)					Average (°)
Control	73	73	71	71	72	72
Air plasma	27	25	27	26	26	26
Control + silane	83	83	83	83	83	83
Air plasma + silane	63	63	62	61	62	62

in Fig. 5. This makes the measurement of the SWCNT coating thickness difficult. It is estimated that each dip coating adds around tens of nanometers of SWCNT to the PET surface. We have also found SWCNT/conductive polymer composite provides better surface quality and better transparency–conductivity combination. Details on this are reported in Ref. [23].

Conclusions

By treating PET surfaces with air plasma and silane solution, highly transparent and conductive SWCNT thin films can be efficiently deposited using solution fabrication method. The mechanism behind this is that air plasma treatment significantly improves the coverage rate of silane on PET surface, which then facilitates the coating of CNT thin films.

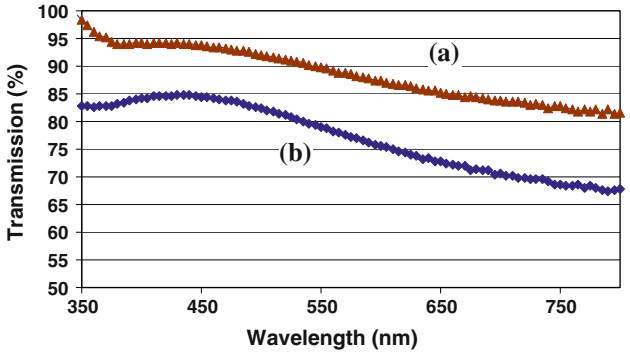

Fig. 4 Typical transmission spectra of SWCNT based thin films deposited on PET surface by solution dipping method. **a** One dip; **b** Two dips

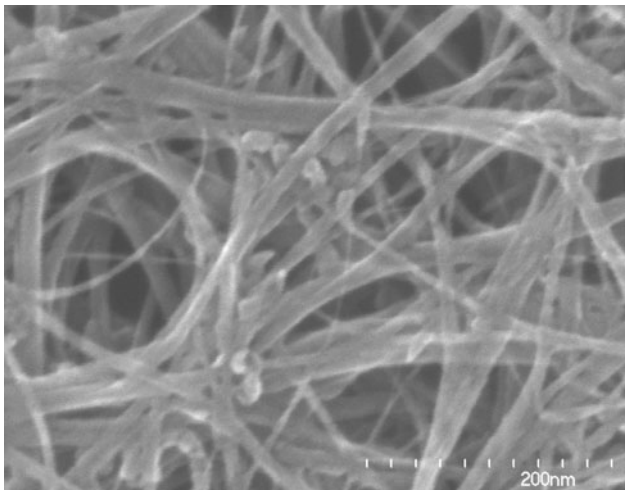

Fig. 5 Typical SEM picture of pure SWCNT coating on PET surface

Acknowledgement This work was supported by the Sustainable Development Technology Canada.

References

1. Na S, Kim S, Jo J, Kim D (2008) Adv Mater 20:4061
2. Lewis J, Grego S, Chalamala B, Vick E, Temple D (2004) Appl Phys Lett 85:3450
3. Cairns DR, Witte RP, Sparacin DK, Sachsman SM, Paine DC, Crawford GP (2000) Appl Phys Lett 76:1425
4. Ng MHA, Hartadi LT, Tan H, Poa CHP (2008) Nanotechnology 19:205703
5. Zhang M, Fang S, Zakhidov AA, Lee SB, Aliev AE, Williams CD, Atkinson KR, Baughman RH (2005) Science 309:1215
6. Rowell MW, Topinka MA, McGehee MD (2006) Appl Phys Lett 88:233506
7. Feng Y, Ju X, Feng W, Zhang H, Cheng Y, Liu J, Fujii A, Ozaki M, Yoshino K (2009) Appl Phys Lett 94:123302
8. Kaempgen M, Duesberg GS, Roth S (2005) Appl Surf Sci 252:425
9. Boccaccini AR, Cho J, Roether JA, Thomas BJC, Minay EJ, Shaffer MSP (2006) Carbon 44:3149
10. Sreekumar TV, Liu T, Kumar S (2003) Chem Mater 15:175
11. Wu Z, Chen Z, Du X, Logan JM, Sippel J, Nikolou M, Kamaras K, Reynolds JR, Tanner DB, Hebard AF, Rinzler AG (2004) Science 305:1273
12. Geblinger N, Thiruvengadathan R, Regev O (2007) Compos Sci Technol 67:895
13. Yu X, Rajamani R, Stelson KA, Cui T (2006) Sens Actuators A 132:626
14. Andrade MJ, Lima MD, Skakalova V, Bergmann CP, Roth S (2007) Phys Status Solidi 1:178
15. http://srdata.nist.gov/xps
16. Briggs D, Beamson G (1992) High resolution XPS of organic polymers: the scienta ESCA300 database. Wiley, New York
17. Louette P, Bodino F, Pireaux JJ (2005) Surf Sci Spectra 12:1
18. Le QT, Pereaux JJ (1997) J Adhes Sci Technol 11:735
19. Yang L, Chen J, Guo Y, Zhang Z (2009) Appl Surf Sci 255:4446
20. Wu S (1982) Polymer interface and adhesion. M. Dekker, New York
21. Zhang H-S, Komvopoulos K (2009) J Appl Phys 105:083305
22. Zhang H-S, Komvopoulos K (2009) J Appl Phys 106:093504
23. Xiao G, Tao Y, Lu J, Zhang Z (2010) Thin Solid Films 518:2822